JACC: CARDIOVASCULAR INTERVENTIONS
VOL. 7, NO. 1, 2014

ISSN 1936-8798/$36.00
PUBLISHED BY ELSEVIER INC.
http://dx.doi.org/10.1016/j.jcin.2013.05.024

A Novel Noninvasive Technology for Treatment Planning Using Virtual Coronary Stenting and Computed Tomography-Derived Computed Fractional Flow Reserve

Kyung-Hee Kim, MD,* Joon-Hyung Doh, MD,† Bon-Kwon Koo, MD,* James K. Min, MD,‡ Andrejs Erglis, MD,§ Han-Mo Yang, MD,* Kyung-Woo Park, MD,* Hae-Young Lee, MD,* Hyun-Jae Kang, MD,* Yong-Jin Kim, MD,* Sung Yun Lee, MD,† Hyo-Soo Kim, MD*

Seoul and Goyang, Republic of Korea; Los Angeles, California; and Riga, Latvia

Objectives This study sought to determine whether computational modeling can be used to predict the functional outcome of coronary stenting by virtual stenting of ischemia-causing stenoses identified on the pre-treatment model.

Background Computed tomography (CT)-derived fractional flow reserve (FFR) is a novel noninvasive technology that can provide computed (FFR_{CT}) using standard coronary CT angiography protocols.

Methods We prospectively enrolled 44 patients (48 lesions) who had coronary CT angiography before angiography and stenting, and invasively measured FFR before and after stenting. FFR_{CT} was computed in blinded fashion using coronary CT angiography and computational fluid dynamics before and after virtual coronary stenting. Virtual stenting was performed by modification of the computational model to restore the area of the target lesion according to the proximal and distal reference areas.

Results Before intervention, invasive FFR was 0.70 ± 0.14 and noninvasive FFR_{CT} was 0.70 ± 0.15. FFR after stenting and FFR_{CT} after virtual stenting were 0.90 ± 0.05 and 0.88 ± 0.05, respectively ($R = 0.55$, $p < 0.001$). The mean difference between FFR_{CT} and FFR was 0.006 for pre-intervention (95% limit of agreement: −0.27 to 0.28) and 0.024 for post-intervention (95% limit of agreement: −0.08 to 0.13). Diagnostic accuracy of FFR_{CT} to predict ischemia (FFR $\leq$0.8) prior to stenting was 77% (sensitivity: 85.3%, specificity: 57.1%, positive predictive value: 83%, and negative predictive value: 62%) and after stenting was 96% (sensitivity: 100%, specificity: 96% positive predictive value: 50%, and negative predictive value: 100%).

Conclusions Virtual coronary stenting of CT-derived computational models is feasible, and this novel noninvasive technology may be useful in predicting functional outcome after coronary stenting. (Virtual Coronary Intervention and Noninvasive Fractional Flow Reserve [FFR]; NCT01478100)
(J Am Coll Cardiol Intv 2014;7:72–8) © 2014 by the American College of Cardiology Foundation

From the *Department of Medicine, Seoul National University Hospital, Seoul, Republic of Korea; †Department of Medicine, Inje University Ilsan Paik Hospital, Goyang, Republic of Korea; ‡Department of Medicine, Cedars-Sinai Heart Institute, Cedars-Sinai Medical Center, Los Angeles, California; and the §Department of Medicine, Pauls Stradins Clinical University Hospital, Riga, Latvia. This study was supported by grants from the Innovative Research Institute for Cell Therapy (A062260); the Korea Healthcare Technology Research and Development Project, Ministry of Health and Welfare, Republic of Korea (A102065, A070001); and the Seoul National University Hospital Research Fund (03-2010-0270). The fractional flow reserve from coronary computed tomographic angiography analysis was performed by HeartFlow, Inc. Dr. Min has received research support from GE Healthcare and Philips Healthcare; has served on the medical advisory boards of GE Healthcare, Arineta, AstraZeneca, and Bristol-Myers Squibb; has served on the Speakers' Bureau of GE Healthcare; has received consulting fees from AstraZeneca, Bristol-Myers Squibb, and HeartFlow Inc.; and has equity interest in TC3 and MDDX. All other authors have reported that they have no relationships relevant to the contents of this paper to disclose. Drs. K.-H. Kim and Doh contributed equally to this paper.

Manuscript received February 15, 2013; revised manuscript received May 20, 2013, accepted May 24, 2013.

Revascularization of coronary artery stenoses that induce ischemia can improve the functional status and clinical outcome of patients with coronary artery disease (1,2). Measurement of fractional flow reserve (FFR) during invasive coronary angiography is the gold standard for the diagnosis of ischemia-causing stenoses and can enhance clinical decision making and reduce healthcare costs (3,4). Coronary computed tomographic angiography (cCTA) is a commonly used noninvasive test that can provide accurate anatomical information on coronary artery disease (5,6). Previous studies, however, have shown that stenosis severity interpreted on cCTA does not match well with functional severity evaluated by invasive FFR (7).

See page 79

Recently, application of computational fluid dynamics technology to cCTA images has enabled computation of coronary artery blood flow and pressure, and calculation of lesion-specific FFR without the need for an invasive procedure (8). FFR can be computed from typically acquired cCTA scans without any additional image acquisition, modification of cCTA protocols, or administration of medications. Previous studies (9,10) suggest that computation of FFR from cCTA (FFR_{CT}) can identify patients with functionally significant coronary lesions prior to invasive cardiac catheterization. The same computational modeling technology allows for modification of the coronary flow model to eliminate an ischemia-causing stenosis, thus enabling "virtual stenting" of a coronary lesion. The resulting re-calculation of coronary blood flow and FFR_{CT} can, in turn, serve to predict hemodynamic effect of coronary stenting in a lesion-specific manner. Such prediction of revascularization benefit (or lack thereof) may be a useful tool for patient or lesion selection and treatment planning prior to invasive procedures.

The purpose of this study is to determine whether virtual stenting of coronary stenoses identified on CT-based computational models can predict functional status of coronary lesions after stenting using measured FFR as the reference standard.

Methods

Study design and population. At 3 centers, 44 patients who had functionally significant coronary stenoses (35 men, mean age 65 years) with available pre-intervention cCTA and pre- and post-intervention FFR were enrolled. All patients were stable adults ≥18 years with suspected or known coronary artery disease who had undergone cCTA, were identified as having a ≥50% stenosis in a major coronary artery (≥2.0 mm diameter), and who underwent clinically indicated invasive coronary angiography with FFR measurement. Coronary calcium scoring was not performed at the time of cCTA, although no patient was excluded based on the upper threshold of qualitative coronary calcification, heart rate, or body mass index. Performance and timing of the invasive coronary angiography or FFR was at the discretion of the treating physician, but study cases were limited to those in which cCTA and invasive angiography was performed within 45 days without an intervening coronary event. The study protocol was approved by the institutional review boards of each participating center and all patients gave written informed consent.

cCTA and invasive coronary procedures. Each center performed cCTA in accordance with the Society of Cardiovascular Computed Tomography guidelines on performance of cCTA using a variety of different CT scanner platforms (Lightspeed VCT, GE Healthcare, Milwaukee, Wisconsin; Somatom Sensation and Definition CT, Siemens, Forchheim, Germany; Brilliance 256 and 64, Philips, Surrey, United Kingdom; Aquilion One and 64, Toshiba, Otawara, Japan). cCTA were performed by retrospective electrocardiographic helical or prospective electrocardiography-triggered methods. Oral metoprolol was administered for any patient with a heart rate ≥65 beats/min. Immediately before image acquisition, 0.2 mg sublingual nitroglycerin was administered. During the cCTA acquisition, 80 to 140 cc of iodinated contrast was injected followed by a 50-cc saline flush. Contrast timing was performed to optimize uniform contrast enhancement of the coronary arteries. The scan parameters were as follows: 64/256/320 × 0.5/0.625/0.750 mm collimation; tube voltage 100 or 120 mV; effective 400 to 650 mA. Dose reduction strategies—including electrocardiogram-gated tube current modulation and reduced tube voltage—were employed whenever feasible.

Abbreviations and Acronyms

cCTA = coronary computed tomographic angiography

FFR = fractional flow reserve

FFR_{CT} = computed fractional flow reserve from coronary computed tomographic angiography

LAD = left anterior descending

TIMI = Thrombolysis In Myocardial Infarction

Coronary angiography and percutaneous coronary intervention were performed by standard techniques. The revascularization strategy, including the size of balloon and coronary stent, was left to the discretion of the operators. FFR was measured using a 0.014-inch pressure-monitoring guidewire (Pressure Wire Certus, St. Jude Medical Systems, Uppsala, Sweden) with the pressure sensor at the same location before and after coronary stenting. Maximal hyperemia was induced with a continuous intravenous infusion of adenosine at the rate of 140 μg/kg/min. FFR was calculated as the ratio of the mean distal pressure to the mean aortic pressure during maximal hyperemia. An FFR ≤0.8 was considered diagnostic of lesion-specific ischemia. FFR was measured in a blinded fashion, without knowledge of FFR_{CT} values.

FFR_{CT} and virtual stenting. FFR_{CT} computation was performed without knowledge of pre- or post-stent FFR values by HeartFlow, Inc. (Redwood City, California) as described previously (9). To illustrate briefly, 3-dimensional models of the coronary tree were reconstructed using custom methods applied to cCTA data, and coronary flow and pressure were simulated using computational fluid dynamics principles (8). Resting flow was estimated from the myocardial mass, and resting microcirculatory resistance was distributed according to the size of the feeding vessel. A lumped parameter model representing the resistance to flow during simulated maximal hyperemia was applied to each coronary branch of the cCTA model, and FFR_{CT} was computed for the entire coronary tree. The point on the model that corresponded to the location of the measured FFR was then selected and results were recorded. The pre-stent computational model was then marked with the location of the stent used to treat the patient. Analysts, blinded as to the results of treatment and to all FFR measurements, then performed virtual coronary intervention by modifying the computational model in the region of the stent to enlarge the lumen of the treated coronary segment according to the proximal and distal reference areas. Computational analysis of hyperemic coronary flow and pressure for the entire heart model was then repeated to determine post-treatment FFR_{CT}. A core lab scientist, blinded to the results of measured FFR, then selected the point on the computational model that matched the location of post-stent FFR measurement to determine the corresponding FFR_{CT} value beyond that stenosis (Fig. 1).

Statistical analyses. Categorical data are expressed as the number and percentage, whereas continuous variables are presented as the mean ± SD. Mean values were compared using paired and unpaired Student *t* tests as appropriate. Spearman rank correlation was used to assess the relationship between FFR and FFR_{CT}. The Bland-Altman analysis and intraclass correlation coefficient were used to assess the degree of agreement between FFR and FFR_{CT}. Statistical analyses were performed using SPSS for Windows (version 17, SPSS Inc., Chicago, Illinois).

Results

Clinical, angiographic, and procedural characteristics. The median time between cCTA and invasive coronary angiography was 12 days (range: 2 to 40). Table 1 provides the clinical, angiographic, and procedural characteristics of the 44 patients. Mean left ventricular ejection fraction was 63.1 ± 7.4%, and 5 patients (10%) had a history of previous myocardial infarctions. The target vessels in patients with previous myocardial infarction were non-infarct-related vessels. Forty-eight coronary lesions were stented; mean stent diameter was 3.1 ± 0.4 mm and mean stent length was 26.0 ± 10.1 mm. All treated patients had TIMI (Thrombolysis In Myocardial Infarction) flow grade 3 after stenting. After stenting, angiographic percentage of diameter stenosis

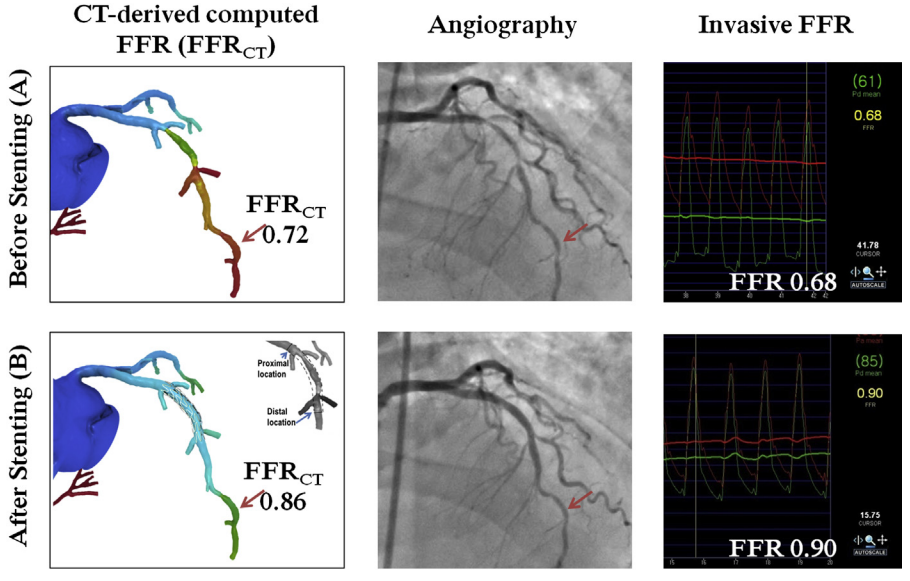

Figure 1. Invasive and Noninvasive Functional Assessment Before and After Revascularization

(A) Noninvasive fractional flow reserve (FFR) from coronary computed tomographic angiography data (FFR_{CT}) of the left anterior descending (LAD) coronary artery was 0.72. Invasive coronary angiography and FFR confirmed the functionally significant LAD stenosis. **(B)** FFR_{CT} demonstrated no ischemia in the LAD after virtual stenting, with a computed value of 0.86. Invasive FFR after stent implantation was 0.90.

Table 1. Clinical, Angiographic, and Procedural Characteristics

Age, yrs	65.0 ± 9.1
Male	35 (80)
Body mass index, kg/m^2	24.4 ± 2.6
Diabetes	13 (29)
Hypertension	36 (81)
Hyperlipidemia	28 (63)
Previous myocardial infarction	5 (10)
LV ejection fraction	63.1 ± 7.4
Lesion locations	
Left anterior descending artery	35 (73)
Left circumflex artery	5 (10)
Right coronary artery	8 (17)
Quantitative coronary angiography	
Before stenting	
Reference diameter, mm	2.96 ± 0.68
Minimal lumen diameter, mm	1.07 ± 0.51
Percentage of diameter stenosis	64.5 ± 14.1
Lesion length, mm	21.5 ± 13.5
After stenting	
Reference diameter, mm	2.96 ± 0.45
Minimal lumen diameter, mm	2.64 ± 0.49
Percentage of diameter stenosis	10.1 ± 8.5
Stent length, mm	26.0 ± 10.1
Stent diameter, mm	3.1 ± 0.42

Values are mean ± SD or n (%).
LV = left ventricular.

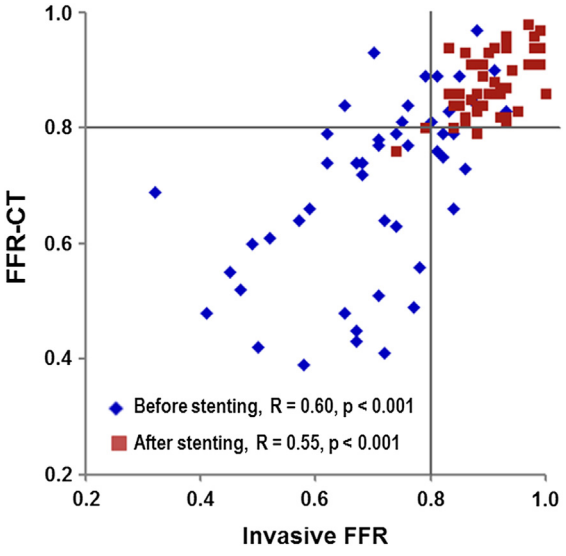

Figure 2. Correlations of FFR and FFR_{CT} Before and After Coronary Intervention

A good correlations (R = 0.60 before stenting and R = 0.55 after stenting) are observed before and after coronary intervention. Abbreviations as in Figure 1.

improved to 10.1 ± 8.5% from a pre-stent diameter stenosis of 64.5 ± 14.1%.

Comparison of FFR_{CT} and invasively measured FFR. Measured FFR prior to intervention was 0.70 ± 0.14 and increased to 0.90 ± 0.05 after stenting. Computed FFR_{CT} prior to intervention was 0.70 ± 0.15 and increased to 0.88 ± 0.05 after virtual coronary stenting. There was a positive correlation between FFR and FFR_{CT} before (R = 0.60, p < 0.001) and after intervention (R = 0.55, p < 0.001) (Fig. 2). The mean difference between FFR_{CT} and FFR was 0.006 for pre-intervention (95% limit of agreement: −0.27 to 0.28) and 0.024 for post-intervention (95% limit of agreement: −0.08 to 0.13) (Fig. 3). Intraclass correlation coefficient was 0.71 (p < 0.001).

FFR_{CT} for the prediction of residual ischemia. Residual ischemia after stenting was found in 2 patients by FFR and predicted in 4 patients by FFR_{CT}. In the 2 patients with false positives, FFR was 0.88 and FFR_{CT} was 0.79 in 1 patient, and FFR was 0.84 and FFR_{CT} was 0.80 in the other patient. Diagnostic accuracy of FFR_{CT} to predict ischemia (FFR ≤0.8) prior to stenting was 77% (sensitivity: 85.3%, specificity: 57.1%, positive predictive value: 83%, and negative predictive value: 62%) and after stenting was 96% (sensitivity: 100%, specificity: 96%, positive predictive value: 50%, and negative predictive value: 100%) (Fig. 4).

Figure 5 illustrates the potential of this novel technology. In one case (Fig. 5A), the operator needed to decide whether to implant a stent from the distal left main segment to cover fully the ostium of the left anterior descending (LAD) coronary artery to relieve the ischemia. A stent was implanted without covering the LAD ostium, and invasively measured FFR after stenting was 0.74. Consistent with this finding, FFR_{CT} after virtual stenting without covering the LAD ostial lesion was 0.76, which was improved to 0.81 after virtual treatment of the whole LAD lesion including the ostium. In another case (Fig. 5B), understanding the functional significance of the left circumflex ostial lesion is critical in planning the treatment strategy. Although the lesion was significant by both angiography and cCTA, FFR_{CT} after virtual stenting of the distal left circumflex lesion was 0.83. During the invasive procedure, it was found that the ischemia was relieved by stenting the distal lesion with a post-stent FFR of 0.88.

Discussion

This study demonstrates that computational modeling of the coronary tree using cCTA images and virtual stenting is feasible and can help to predict the functional outcomes of stenting prior to invasive coronary angiography. This novel technique provides a noninvasive method for planning optimal treatment strategies in a patient- and lesion-specific manner before invasive procedures. These results—though needing validation in a larger cohort—represent initial findings

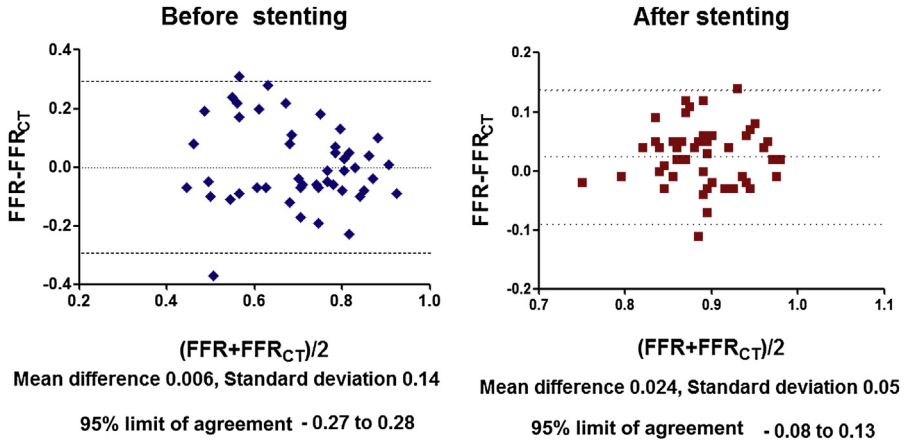

Figure 3. Bland-Altman Plot for the Agreement Between FFR_{CT} and FFR Before and After Stenting

The mean difference between FFR_{CT} and FFR is 0.006 for pre-intervention (95% limit of agreement: −0.27 to 0.28) and 0.024 for post-intervention (95% limit of agreement: −0.08 to 0.13). Abbreviations as in Figure 1.

that demonstrate the potential of this technology to not only diagnose lesion-specific ischemia but also to predict the therapeutic benefit of coronary revascularization.

Whereas cCTA can be helpful in identifying patients with coronary stenosis and selecting patients for invasive angiography, it is well known that the functional significance of stenosis cannot be accurately assessed by cCTA (7,11–13). In the present study, we sought to assess the accuracy of treatment planning using the computational model to simulate a virtual stent and to determine whether computation of anticipated post-stent FFR_{CT} could predict the success of stenting prior to the invasive procedures. It is important to note that virtual stenting is performed by modification of the computational model derived from the original cCTA taken before the invasive procedure, and that post-stent FFR can be predicted from this same model without any additional noninvasive or invasive procedures. We found that FFR_{CT} had a diagnostic accuracy of 96% in predicting or ruling out myocardial ischemia after stenting as defined by a post-stent FFR of >0.80. The mean difference between FFR after stenting and FFR_{CT} after virtual stenting was 0.02 ± 0.05. Thus, it appears that comprehensive planning of a revascularization strategy and selection of the optimal target coronary lesion(s) for revascularization is possible using this novel technology, which can provide both anatomical and functional information for each lesion before the invasive procedure. This technique can be especially helpful for determining the revascularization strategy in patients with complex disease. For example, in patients with serial stenoses, even using invasive FFR, the true functional significance of each stenosis cannot be precisely assessed until the elimination of the other stenoses (14,15). However, it is possible to discriminate the functional significance of each stenosis using virtual stenting and computed FFR_{CT}. Therefore, clinical application of this noninvasive "all-in-one" diagnostic and treatment planning approach may reduce clinically unnecessary interventions, procedural time, radiation dose, and costs. Importantly, we did not examine the potential diagnostic performance of FFR_{CT} to identify lesions that may be best treated by medical therapy and/or coronary artery bypass

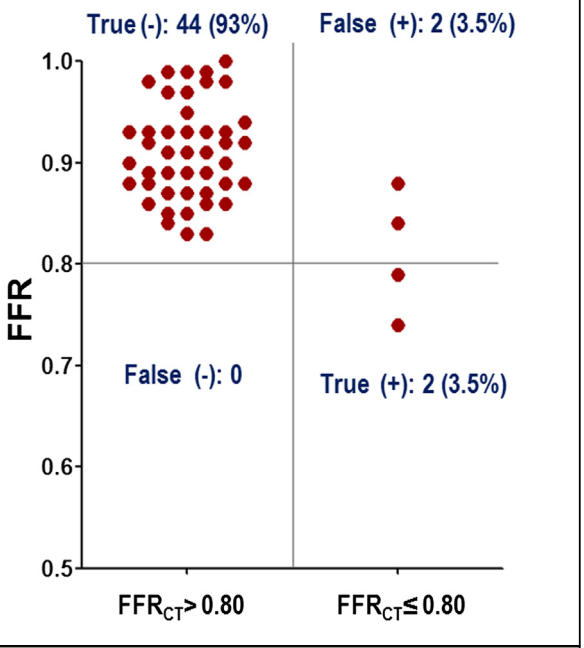

Figure 4. Diagnostic Performance of FFR_{CT} After Virtual Stenting to Predict the Presence of Ischemia After Stenting

Diagnostic accuracy of FFRCT to predict ischemia prior to stenting is 77% and after stenting is 96%. Abbreviations as in Figure 1.

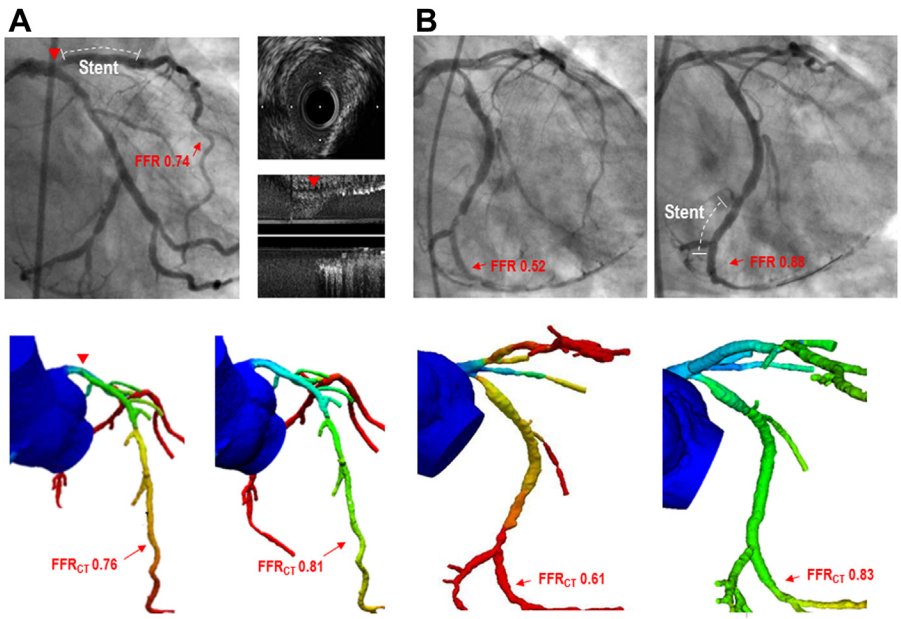

Figure 5. Cases Illustrating the Potential of Noninvasive Treatment Planning Using Virtual Stenting and FFR$_{CT}$

(A) Post-stenting FFR was 0.74, as the ostial lesion **(red arrowhead)** of LAD was not covered. Intravascular ultrasound showed the uncovered plaque at the ostium of LAD **(upper right)**. FFR$_{CT}$ without covering the LAD ostial lesion was 0.76, but it was 0.81 after treating the whole LAD lesion. **(B)** Post-stent FFR in the left circumflex (LCX) artery was 0.88 despite an angiographically significant stenosis at the ostium of LCX. As part of pre-procedural planning prior to an invasive procedure, functional significance of the ostial lesion could be assessed via FFR$_{CT}$ after virtual stenting of distal LCX lesion (post-virtual stenting FFR$_{CT}$ 0.83). Abbreviations as in Figure 1.

graft. Whereas the FFR$_{CT}$ is hypothetically capable of determination of these findings, it remains unknown whether FFR$_{CT}$ can determine post-medical therapy and/or post–coronary artery bypass graft FFR with as high a diagnostic performance as reported in this study of percutaneous revascularization. Future diagnostic and outcomes studies evaluating these concepts now appear warranted.

Study limitations. First, the number of patients enrolled in this study was relatively small, with no systematic derivation/validation cohorts. Future studies doing so will be needed to corroborate these initial study results and, until then, these findings should be considered as "proof-of-concept." Second, because this technology depends on the image quality of cCTA, it can be applied only to patients with diagnostic quality cCTA images obtained prior to invasive catheterization. Third, as this technology does not incorporate the microvascular injury during percutaneous coronary intervention, the accuracy of post-stent FFR$_{CT}$ can be lower in patients with severe microvascular injury during stent implantation. Fourth, as the FFR calculation is based on resting coronary anatomy, possible anatomical changes during actual stress cannot be reflected. However, to minimize this influence, all patients were given sublingual nitroglycerin immediately before cCTA. Finally, FFR$_{CT}$ is a new technology and further studies are needed to determine its clinical utility. Nonetheless, this novel technique is promising, and the present study demonstrates its potential as a noninvasive method for treatment planning prior to invasive coronary angiography and interventional procedures.

Conclusions

Treatment planning using noninvasive FFR$_{CT}$ and virtual stenting is feasible and may be helpful in determining optimal revascularization strategies before invasive procedures.

Reprint requests and correspondence: Dr. Bon-Kwon Koo, Division of Cardiology, Department of Internal Medicine, Seoul National University College of Medicine, 101 Daehak-ro, Jongno-gu, Seoul 110-744, Republic of Korea. E-mail: bkkoo@snu.ac.kr.

REFERENCES

1. Shaw LJ, Berman DS, Maron DJ, et al., for the COURAGE Investigators. Optimal medical therapy with or without percutaneous coronary intervention to reduce ischemic burden: results from the Clinical Outcomes Utilizing Revascularization and Aggressive Drug Evaluation (COURAGE) trial nuclear substudy. Circulation 2008;117:1283–91.
2. Erne P, Schoenenberger AW, Burckhardt D, et al. Effects of percutaneous coronary interventions in silent ischemia after myocardial infarction: the SWISSI II randomized controlled trial. JAMA 2007; 297:1985–91.
3. Fearon WF, Bornschein B, Tonino PA, et al., for the FAME Study Investigators. Economic evaluation of fractional flow reserve-guided

percutaneous coronary intervention in patients with multivessel disease. Circulation 2010;122:2545–50.
4. De Bruyne B, Pijls NH, Kalesan B, et al., for the FAME 2 Trial Investigators. Fractional flow reserve-guided PCI versus medical therapy in stable coronary disease. N Engl J Med 2012;367:991–1001.
5. Min JK, Shaw LJ, Berman DS. The present state of coronary computed tomography angiography: a process in evolution. J Am Coll Cardiol 2010;55:957–65.
6. Pregowski J, Kepka C, Kruk M, et al. Comparison of usefulness of percutaneous coronary intervention guided by angiography plus computed tomography versus angiography alone using intravascular ultrasound end points. Am J Cardiol 2011;108:1728–34.
7. Meijboom WB, Van Mieghem CA, van Pelt N, et al. Comprehensive assessment of coronary artery stenoses: computed tomography coronary angiography versus conventional coronary angiography and correlation with fractional flow reserve in patients with stable angina. J Am Coll Cardiol 2008;52:636–43.
8. Kim HJ, Vignon-Clementel IE, Coogan JS, Figueroa CA, Jansen KE, Taylor CA. Patient-specific modeling of blood flow and pressure in human coronary arteries. Ann Biomed Eng 2010;38:3195–209.
9. Koo BK, Erglis A, Doh JH, et al. Diagnosis of ischemia-causing coronary stenoses by noninvasive fractional flow reserve computed from coronary computed tomographic angiograms: results from the prospective multicenter DISCOVER-FLOW (Diagnosis of Ischemia-Causing Stenoses Obtained Via Noninvasive Fractional Flow Reserve) study. J Am Coll Cardiol 2011;58:1989–97.
10. Min JK, Leipsic J, Pencina MJ, et al. Diagnostic accuracy of fractional flow reserve from anatomic CT angiography. JAMA 2012;308:1237–45.
11. Tonino PA, De Bruyne B, Pijls NH, et al., for the FAME Study Investigators. Fractional flow reserve versus angiography for guiding percutaneous coronary intervention. N Engl J Med 2009;360:213–24.
12. Blankstein R, Di Carli MF. Integration of coronary anatomy and myocardial perfusion imaging. Nat Rev Cardiol 2010;7:226–36.
13. Bamberg F, Becker A, Schwarz F, et al. Detection of hemodynamically significant coronary artery stenosis: incremental diagnostic value of dynamic CT-based myocardial perfusion imaging. Radiology 2011;260:689–98.
14. De Bruyne B, Pijls NH, Heyndrickx GR, Hodeige D, Kirkeeide R, Gould KL. Pressure-derived fractional flow reserve to assess serial epicardial stenoses: theoretical basis and animal validation. Circulation 2000;101:1840–7.
15. Pijls NH, De Bruyne B, Bech GJ, et al. Coronary pressure measurement to assess the hemodynamic significance of serial stenoses within one coronary artery: validation in humans. Circulation 2000;102:2371–7.

Key Words: coronary computed tomographic angiography ■ computational fluid dynamics ■ fractional flow reserve.